high-performance liquid chromatography and electrospray ionization tandem mass spectrometry (HPLC/ESI-MS/MS).[16] Now, more than 100 different analytes with amino groups can be measured within 10 minutes by the combination of the precolumn derivatization and HPLC/ESI-MS/MS techniques. This method represents an alternative to traditional amino acid analysis techniques. The aim of this study was to reveal and describe the amino acid profiles in human tear fluids since this new method now makes it possible to analyze samples in trace amounts (below 0.5 μL) and with a superior reproducibility.[16] In addition, the possible physiological and pharmacologic function of amino acids will be discussed.

METHODS

• NORMAL VOLUNTEER SUBJECTS: Enrolled in this study were normal volunteer subjects with no corneal-, conjunctival-, or lacrimal-system abnormalities as assessed by slit-lamp examination. Free amino acids were evaluated in blood samples obtained from 11 healthy young male (mean age: 22.9 ± 1.4 years), 6 healthy young female (mean age: 21.0 ± 0.7 years), 6 healthy elderly male (mean age: 69.5 ± 3.8 years), and 11 healthy elderly female (mean age: 71.5 ± 4.0 years) volunteer subjects. Basal tear samples were collected from the young and elderly subjects (n = 31; young male: 10; young female: 6; elderly male: 6; elderly female: 9) and reflex tear samples were also collected from the young subjects (n = 16; male: 10; female: 6). Basal and reflex tear fluid samples (0.5−1.0 μL) were collected from the inferior tear meniscus of each subject using a microcapillary tube. Reflex-tear stimulation was initiated by inserting an applicator into the nose of each subject. Aqueous humor samples were obtained from the elderly subjects (n = 16; male: 6; female: 10) through the use of a 1-mL syringe with a 30-gauge needle prior to cataract surgery, and all of the obtained samples were free of contamination by blood fluids.

• PREPARATION OF TEAR FLUID AND AQUEOUS HUMOR SAMPLES: Each tear sample was transferred into a 0.5-mL sterile microfuge tube and then centrifuged. Supernatants were stored at –70°C until assaying for the amino acid levels. After thawing, 0.5 μL of each tear sample was diluted with 4.5 μL of sterile purified water, and then extracted by the addition of 20 μL of acetonitrile and mixing with a vortex mixer. The samples were centrifuged at 10 000 rpm for 1 minute, and the supernatants were then analyzed. A quantity of 1.0 μL of aqueous humor was used for each sample, with the same dilution as that of the tear fluid.

• PATIENTS WITH OCULAR SURFACE DISEASE AND CORNEAL OR SCLERAL DISEASE: Tear samples were collected from 33 affected subjects composed of 18 subjects with severe ocular surface diseases and 15 subjects with corneal or scleral diseases. Severe ocular surface diseases included Stevens-Johnson syndrome (SJS) (n = 10), chemical injury (n = 4), thermal burn (n = 2), and stem cell deficiency from an unknown cause (n = 2). The corneal or scleral diseases of the other 15 subjects included granular dystrophy (n = 2), band-shaped keratopathy (n = 2), keratoconus (n = 2), bullous keratopathy (n = 2), lattice dystrophy (n = 1), corneal erosion (n = 1), postcorneal infection (n = 2), necrotizing keratitis (n = 1), and scleritis (n = 2). Those 15 subjects were all classified as non–ocular surface disease.

• BIOCHEMICAL ASSAYS OF TEAR FLUID AMINO ACID AND AQUEOUS HUMOR AMINO ACID: For measurement of the amino acid concentration in the tear fluid and aqueous humor samples, we adopted precolumn derivatization with AccQ·Tag (Waters Corporation, Milford, Massachusetts, USA) to increase the ionization efficiency of the adducts before being analyzed by the multiple-reaction monitoring mode of reversed-phase HPLC HP1100 series (Agilent Technologies, Inc, Palo Alto, California, USA) and triple quadrupole tandem mass spectrometry (API4000 LC/MS/MS system; Applied Biosystems, Inc, Foster City, California, USA).[16–18] For derivatization with 20 μL of AccQ·Tag reagent, 20 μL of a deproteinized tear sample was added to 60 μL of 0.2-M borate buffer (pH 8.8) and then heated at 55°C for 10 minutes. The reaction mixture was diluted with 100 μL of 0.2% acetic acid and 5 μL of the mixture was then injected onto the HPLC column (L-Column, 50 mm × 2.0 mm, 3-μm particles; Chemicals Evaluation and Research Institute, Tokyo, Japan) prior to MS detection at a flow rate of 0.25 mL/min.

• BIOCHEMICAL ASSAYS OF PLASMA AMINO ACID: The plasma was separated and deproteinized in a final concentration of 3% sulfosalicylic acid. All samples were stored at –70°C until measurement using HPLC (SRL Inc, Tokyo, Japan). The basic amino acid and related molecules (23 compounds) were measured and used in the analysis. Those compounds are as follows: L-tyrosine (Tyr), Val, Leu, L-methionine (Met), Ile, Gln, L-serine (Ser), L-lysine (Lys), L-asparagine (Asn, AspNH2), L-threonine (Thr), L-alanine (Ala), Glu, His, L-ornithine (Orn), L-cystine (Cys2), L-proline (Pro), L-tryptophan (Trp), Arg, Tau, glycine (Gly), citrulline (Cit), Asp, and L-phenylalanine (Phe).

• STATISTICAL ANALYSIS: Statistical analysis was performed using SPSS statistical analysis software (SPSS Inc, Chicago, Illinois, USA). Hierarchical clustering analysis was performed using JMP7.0 software (SAS Institute, Inc, Cary, North Carolina, USA). The correlations among 23 amino acid concentrations as well as

TABLE 1. Concentration (Mean ± SEM, μM) of Each Amino Acid in the Basal Tears, Reflex Tears, Aqueous Humor, and Plasma of Normal Subjects

	Basal Tear (n = 31)	Reflex Tear (n = 16)	Aqueous Humor (n = 16)	Plasma (n = 34)
Gly	10.7 ± 2.8	14.4 ± 7.1	0.4 ± 0.1	231.3 ± 11.1
Ala	23.8 ± 4.8	19.5 ± 8.5	14.4 ± 2.7	385.5 ± 14.5
Val	3.5 ± 0.9	3.8 ± 1.4	6.7 ± 1.1	244.7 ± 8.5
Leu	10.1 ± 1.9	6.4 ± 1.9	3.3 ± 0.6	125.4 ± 6.1
Ile	1.1 ± 0.3	1.1 ± 0.5	1.5 ± 0.3	68.7 ± 3.6
Ser	14.4 ± 4.2	26.4 ± 13.0	3.9 ± 0.8	113.6 ± 3.3
Thr	5.4 ± 1.2	8.4 ± 3.6	3.5 ± 0.7	127.6 ± 3.8
Met	2.4 ± 0.1	2.2 ± 0.1	0.9 ± 0.2	28.1 ± 1.3
AspNH2 (Asn)	1.4 ± 0.3	1.5 ± 0.7	1.0 ± 0.2	49.6 ± 1.5
GluNH2 (Gln)	42.1 ± 6.8	25.4 ± 6.3	28.7 ± 5.2	589.5 ± 11.0
Pro	8.4 ± 1.4	6.7 ± 1.5	0.5 ± 0.1	180.2 ± 8.5
Phe	10.7 ± 1.9	5.7 ± 1.5	2.8 ± 0.5	63.7 ± 2.0
Tyr	1.3 ± 0.5	1.1 ± 0.5	2.8 ± 0.6	73.5 ± 3.8
Trp	7.1 ± 0.7	6.6 ± 1.0	0.9 ± 0.1	52.9 ± 1.8
Asp	13.2 ± 4.5	18.2 ± 11.6	0.0 ± 0.0	1.8 ± 0.2
Glu	30.2 ± 4.8	20.9 ± 4.8	0.1 ± 0.0	42.3 ± 2.8
Lys	5.7 ± 1.2	3.5 ± 1.2	3.1 ± 0.6	195.7 ± 7.2
Arg	18.7 ± 1.6	14.4 ± 2.5	2.5 ± 0.5	82.7 ± 3.0
His	1.9 ± 0.7	3.2 ± 1.9	1.5 ± 0.3	83.7 ± 2.0
Cit	10.1 ± 0.8	8.2 ± 1.5	1.2 ± 0.2	35.1 ± 1.7
Orn	3.3 ± 1.1	7.1 ± 3.0	0.4 ± 0.1	79.3 ± 4.9
Cys2	1.0 ± 0.2	0.6 ± 0.2	0.3 ± 0.1	49.0 ± 2.4
Tau	195.1 ± 26.9	100.1 ± 18.7	1.2 ± 0.3	57.7 ± 2.0

Ala = L-alanine; Arg = L-arginine; Asp = L-aspartate; AspNH2 (Asn) = L-asparagine; Cit = citrulline; Cys2 = L-cystine; Glu = L-glutamic acid; GluNH2 (Gln) = L-glutamine; Gly = glycine; His = L-histidine; Ile = L-isoleucine; Leu = L-leucine; Lys = L-lysine; Met = L-methionine; Orn = L-ornithine; Phe = L-phenylalanine; Pro = L-proline; Ser = L-serine; Tau = taurine; Thr = L-threonine; Trp = L-tryptophan; Tyr = L-tyrosine; Val = L-valine.

among plasma and/or ophthalmic fluid (basal tear, reflex tear, and aqueous humor) samples were clustered using the Ward method. For the red>gray>blue color system, the depth in the red color or blue color reflected the different degree of values above or below the mean (gray color), respectively. Graphic presentations of box plots were generated using R (R Foundation for Statistical Computing, Vienna, Austria). In each box plot, the top and bottom of the boxes were the first and third quartiles, respectively, and the length of the box represented the inter-quartile range within 50% of the values that were included. The horizontal line within each box represented the median, the vertical lines showed the largest/smallest observation that fell within a distance of 1.5 times the box size from the nearest quartile in the box, and the additional points were considered "extreme" values and are shown separately.

These presentations and analyses were performed based on each of the absolute amino acid concentrations (μM) or relative amino acid composition (percentage), calculated by each amino acid concentration/total 23 amino acid concentrations.

RESULTS

• COMPARISON OF AMINO ACID PROFILES AMONG TEAR FLUID, AQUEOUS HUMOR, AND PLASMA SAMPLES OF NORMAL SUBJECTS: Amino acid concentrations in a trace amount of tear fluids of 0.5 to 1.0 μL were able to be measured reproducibly by HPLC/ESI-MS/MS. The reproducibility of the measurements was confirmed in separate experiments using normal tear fluids. The Table shows the concentrations of each amino acid in the basal tear, the reflex tear, the aqueous humor, and the plasma of normal subjects. A significant difference of amino acid profiles between the tear fluid, the aqueous humor, and the plasma samples was confirmed. The concentration of total amino acids in the tear fluid samples (means ± SEM: 382.1 ± 42.6 μM) was lower than that in the plasma samples (2961.6 ± 63.1 μM) but higher than that in the aqueous humor samples (81.6 ± 15.2 μM). Ala, Val, and Gln were dominant components in the plasma samples (more than 240 μM). Gly, Pro, and Lys were also major components in the plasma samples.

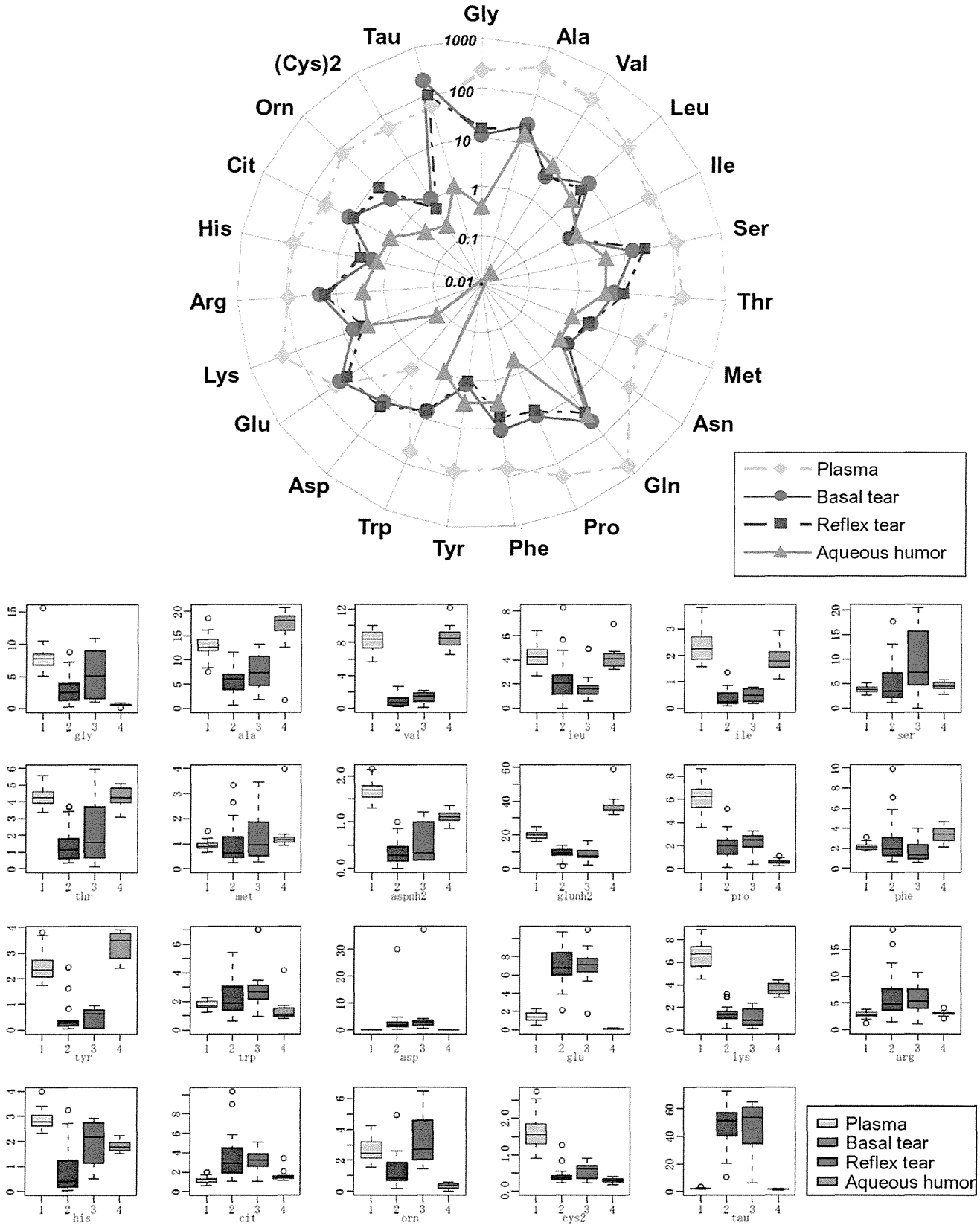

FIGURE 1. The differences of amino acid profiles of normal subjects between basal tear, reflex tear, and aqueous humor samples, compared with that of plasma samples. (Top) Mean values of 23 amino acid concentrations (μM) of basal tear (n = 31) (blue), reflex tear (n = 16) (purple), aqueous humor (n = 16) (red), and plasma (n = 34) (green) samples from normal subjects are shown in

In the tear fluids, Tau, Glu, and Gln were dominant components (more than 25 μM). Arg and Cit were of a higher concentration than other amino acid concentrations, whereas Val, Ile, Met, Asn, Tyr, His, and Orn were of a lower concentration (below 5 μM) (Table, and Figure 1, Top). Notably, the concentrations of Tau and Glu were significantly higher than (3.4 times higher) or comparable with (0.7 times higher) those in plasma samples. Asp also was of a higher value than that in plasma samples. The amino acid concentrations and profiles of the basal tear fluid and reflex tear fluid were found to be similar.

Since it has been shown that the metabolomic profiling of amino acid can be helpful in revealing specific physiological conditions or states, and that the ratios between some specific amino acids can be useful in diagnosing them,[19] we performed some analyses based on not only amino acid concentrations but also relative amino acid composition (Figure 1, Bottom). The composition of amino acid in aqueous humors was rather analogous to that in plasmas, although the levels of Gly, Pro, and Orn were low. In the tear fluid samples, Tau and Glu were of a higher relative amino acid composition (25.0 times higher and 4.9 times higher, respectively; $P < .001$) (Tukey test) than those in the plasma samples, yet the aqueous humor samples were not (Tau: 0.73 times higher, Glu: 0.09 times higher). The relative compositions of Arg and Cit in the tear fluid samples were smaller but statistically significantly higher than those in the plasma and aqueous humor samples. There was no significant difference between the basal tear fluid and reflex tear fluid in 23 relative amino acid compositions (Tukey test).

In an aim to build up a simple visual presentation, the correlations among 23 amino acid concentrations and the relative amino acid composition of 31 basal tear fluid, 16 reflex tear fluid, 16 aqueous humor, and 34 plasma samples were clustered (Figure 2). Plasma samples were clearly clustered at the highest position, followed by tear fluid samples and then aqueous humor samples.

• COMPARISON OF TEAR-FLUID AMINO ACID PROFILES AMONG YOUNG AND ELDERLY VOLUNTEERS: The change of amino acid concentration attributable to aging is known to exist in other body fluids.[20] In this study, a preliminary analysis was carried out on the basal tear fluid and plasma samples of adults that differed by both age and sex. The mean values of 23 amino acids in relation to concentration and composition that were obtained from young male (n = 10), young female (n = 6), elderly male (n = 6), and elderly female (n = 9) normal subjects were examined. The Tukey test showed that the differences were not statistically significant. Hierarchical clustering charts of both the concentration and composition did not exhibit any distinct clustering trends among these 4 groups (data not shown).

• DISTINCTIVE CHANGE OF AMINO ACID PROFILES IN TEAR FLUIDS FROM DISEASED EYES: The difference of amino acid concentrations and profiles among tear fluids from individuals of severe ocular surface disease and non–ocular surface disease was investigated. Means of the 23 amino acid concentrations (μM) from severe ocular surface disease (n = 18) and non–ocular surface disease (n = 15) were shown in a radar chart (Figure 3, Top). The concentrations of amino acid were highly elevated in tear fluids from severe ocular surface disease subjects compared with those from non–ocular surface disease subjects. Four amino acids (Val, Ile, Tyr, and Glu) showed a significant P value of less than .01, and 15 amino acids showed a P value of less than .05 (Student t test). Of important note is the fact that the changes were not restricted to the concentration, but also extended to the amino acid profile, namely composition.

Next, the distribution pattern of the amino acid composition in tear fluids from the severe ocular surface disease subjects was compared with those from the non–ocular surface disease subjects. Amino acid composition (%) of tear fluids from 15 non–ocular surface disease subjects (column 1, left) and 18 severe ocular surface disease subjects (column 2, right) are shown in the box plots (Figure 3, Bottom). The significant changes were the decrease in Arg, Met, and Tau and the increase in Orn, Lys, and Thr in the severe ocular surface disease subjects.

Analysis of the hierarchical clustering of the amino acid profiles of tear fluids from severe ocular surface disease subjects and non–ocular surface disease subjects indicated clear clustering of 12 of the 18 specimens from individuals with severe ocular surface disease when classified on the basis of amino acid composition (Figure 4). Interestingly, the composition-based clustering exhibited 5 distinctive clusters of amino acid, namely Tau/Met/Arg, Asn/Tyr/Val/Ile/Lys, Glu/Gln, Cit/Leu/Phe/Trp/Pro, and Asp/His/Thr/Orn/Ser/Gly/Ala. Decreased amino acid, Tau, Met, and Arg were included in 1 cluster, which suggests a correlation of the metabolism and/or transport of these amino acids in inflammatory eyes.

DISCUSSION

IN THIS STUDY, WE PERFORMED THE SYSTEMATIC QUANTIFICATION of free amino acids in human tear fluids by HPLC/ESI-MS/

the radar chart. (Bottom) Amino acid composition data (percentages) from plasma (n = 34) (green), basal tear (n = 31) (blue), reflex tear (n = 16) (purple), and aqueous humor (n = 16) (red) samples are shown in the box plots. The box represents the first and third quartiles, and the horizontal line within each box represents the median. The vertical lines show the largest/smallest observation, and the additional points are "extreme" values.

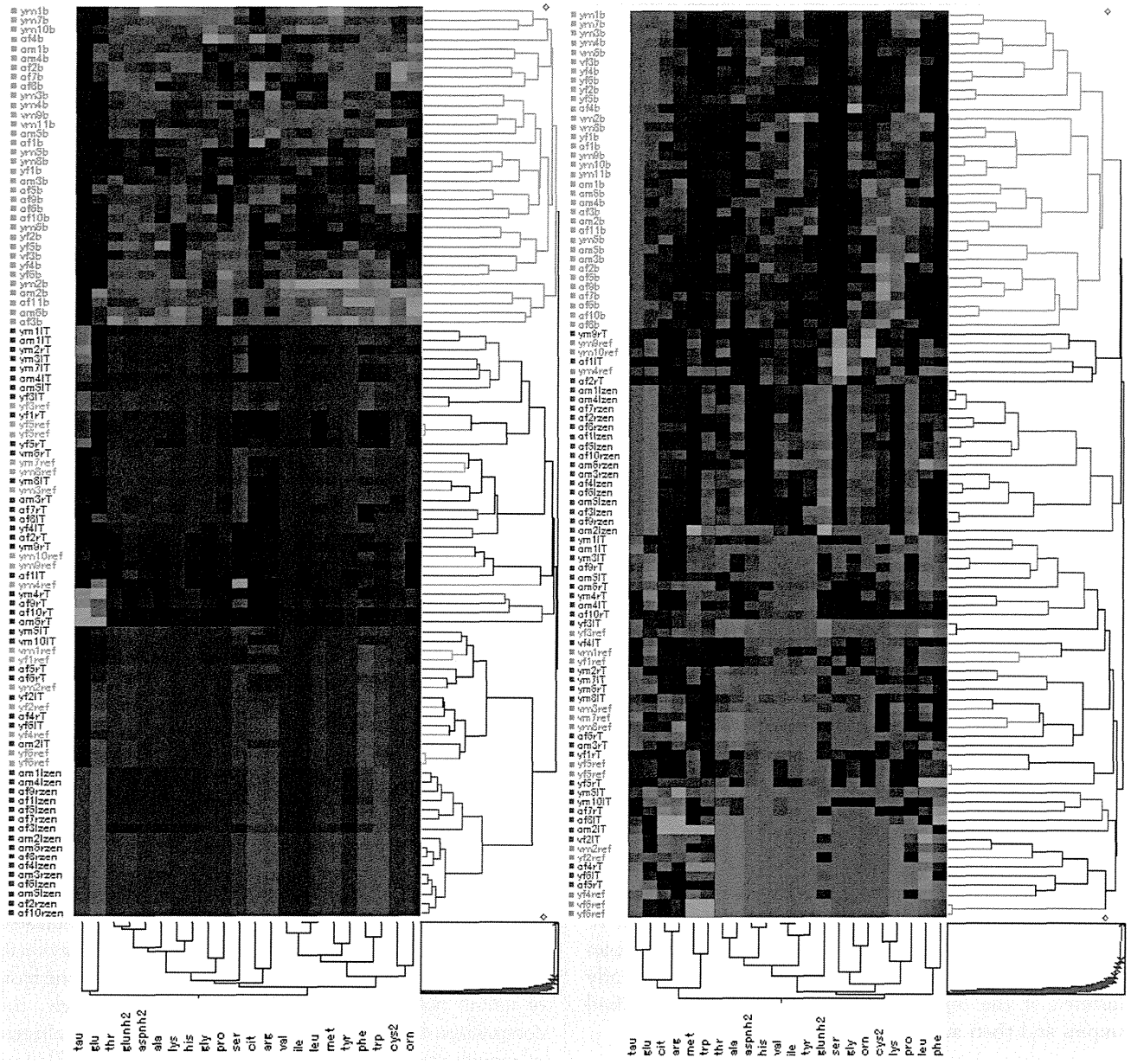

FIGURE 2. Hierarchical clustering of the amino acid profiles of basal tear, reflex tear, aqueous humor, and plasma samples of normal subjects. The correlations among 23 amino acid concentrations (Left) and relative amino acid compositions (Right) of basal tear (n = 31) (blue), reflex tear (n = 16) (green), aqueous humor (n = 16) (purple), and plasma (n = 34) (red) samples were clustered using the Ward method.

MS. The amino acid profiles showed the following characteristics: 1) the amino acid profiles in tear fluids differ from those in aqueous humors and plasmas, 2) the absolute concentrations of Tau, Glu, and Asp in tear fluids are significantly higher than, or comparable with, those in plasma samples, 3) the amino acid profile in the aqueous humor samples was rather analogous to that in the plasma samples, 4) the amino acid profiles of the tear fluid of distinct groups (male vs female, young vs elderly) are similar, and 5) amino acid profiles of tear fluids from severe ocular surface disease subjects differed from those of non–ocular surface disease subjects.

The combination of the precolumn derivatization and HPLC/ESI-MS/MS techniques enabled the analysis of 120 body fluid samples in a single day and may possibly provide an alternative to traditional techniques used for amino acid analysis. From this viewpoint, we theorize that our high-speed, reliable procedure for amino acid analysis will prove to be a useful technique for the diagnosis and management of inherited disorders of amino acid metabolism in the clinical setting. In this study, we discovered that almost all amino acids exist in tear fluid. The plasma concentration of amino acid is the sum of its rates of appearance in and disappearance from plasma, and amino acid appearance

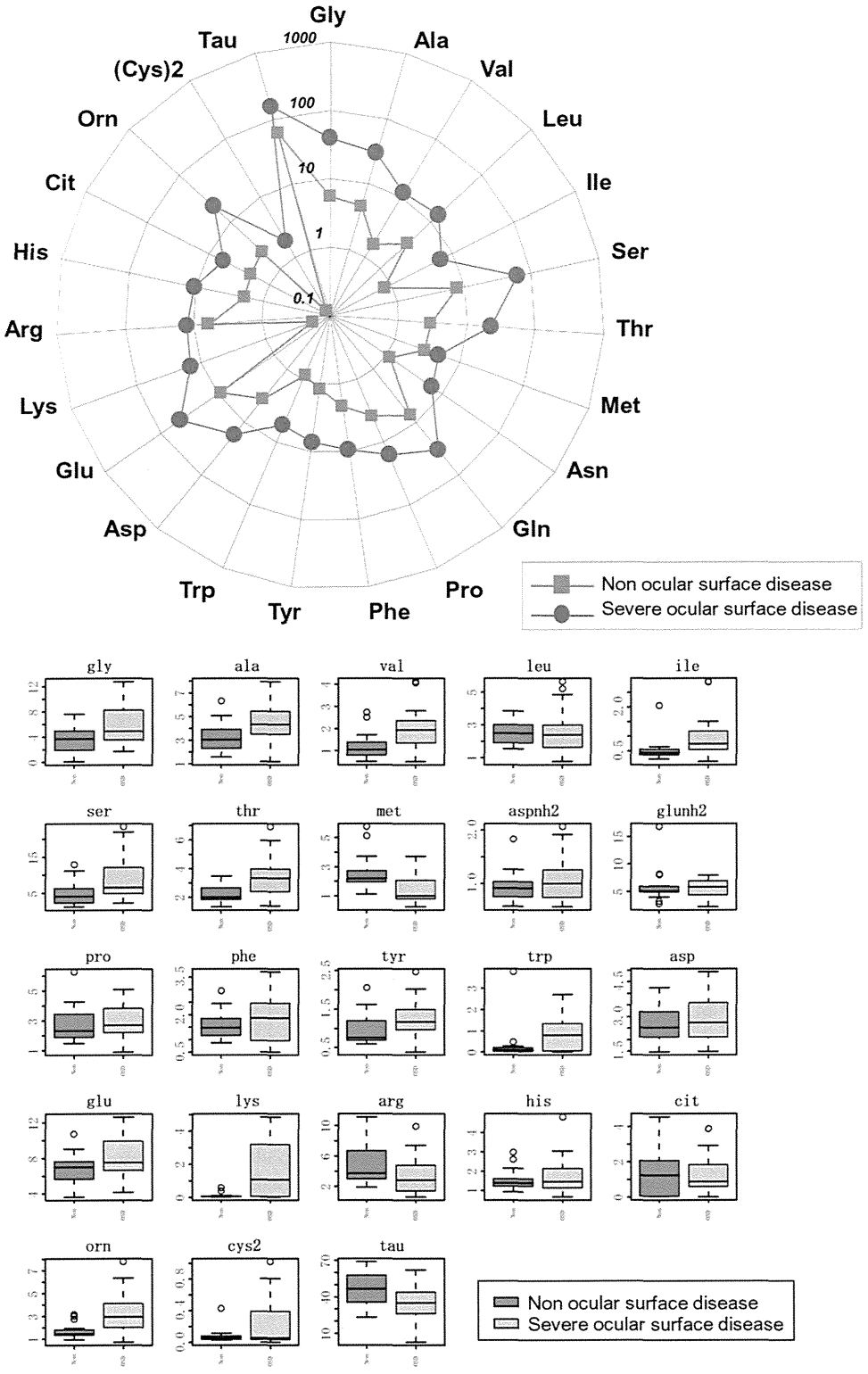

FIGURE 3. The differences of amino acid concentrations between tear fluids from severe ocular surface disease subjects and non-ocular surface disease subjects. (Top) Means values of 23 amino acid concentrations (μM) of tears from severe ocular surface disease subjects (n = 18) (blue) and non-ocular surface disease subjects (n = 15) (red) are shown in the radar chart. (Bottom) Amino acid composition data (percentages) of tears from non-ocular surface disease (n = 15) (red; left) and severe ocular surface disease (n = 18) (blue; right) subjects are shown in the box plots.

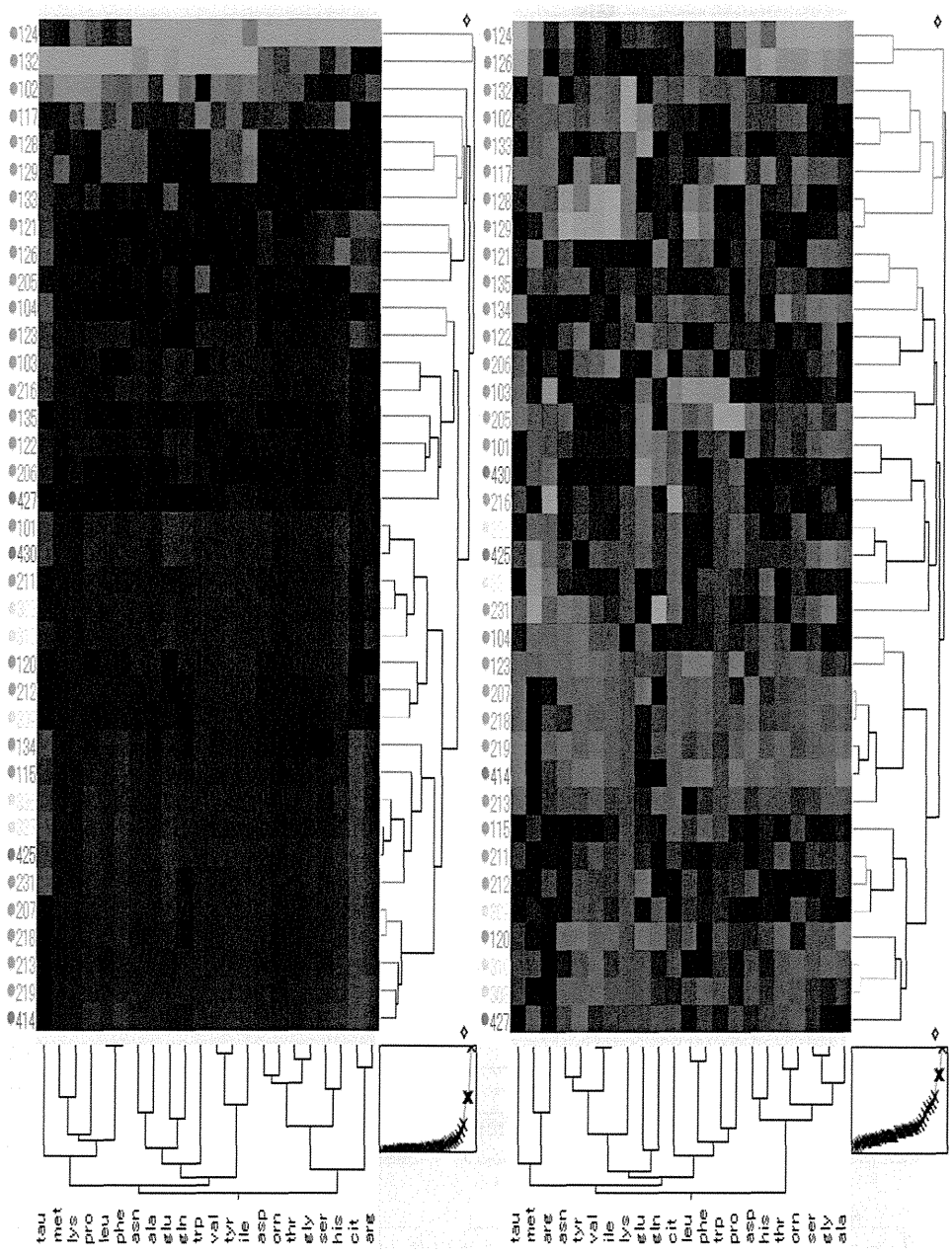

FIGURE 4. Hierarchical clustering of the amino acid profiles of tear fluids from severe ocular surface disease subjects and non–ocular surface disease subjects. The correlations among 23 amino acid concentrations (Left) and relative amino acid compositions (Right) of tear samples from severe ocular surface disease subjects (n = 18) (red) and non–ocular surface disease subjects (n = 15) (green) were clustered using the Ward method. The concentrations and relative composition of 23 amino acids in tear fluids differ from those in plasma and aqueous humor. Analysis of the hierarchical clustering of the amino acid profiles distinguished severe ocular surface diseases from non-ocular surface diseases. Steady-state tear-fluid amino acid profiles might reflect ocular-surface homeostasis and the observed changes of amino acids might have a close relation with the disease conditions on the ocular surface.

and disappearance are tightly regulated. In some circumstances, tissue uptake of amino acid and further metabolism depend on plasma amino acid concentrations. Mere determinations of plasma amino acid concentrations at the basal state (ie, postabsorptive) provide a rather limited amount of information.[21]

Previously, a few reports have presented contradicting results on the amount of limited kinds of free amino acids in human tears.[13,14] In those studies, the quantities found in tear fluids were at a comparable level with those found in plasma, except for the levels of Asp, Glu, and Tau. The high level for Tau in tear fluids was reported previously,[14] and Tau has been identified as a major player in numerous biological functions[22,23] and is involved in the regulation of the proinflammatory responses.[22] Very

recently, it has been demonstrated that Tau plays a key role in regulating epithelial barrier function.[24] In this study, the concentration of Tau was confirmed to be very high in the tear fluid samples compared with that in the plasma samples, consistent with the previous reports. These findings signal the necessity to discriminate the subtle function of Tau under physiological and pathologic environments. Plasma Tau levels are usually high, although decreases are observed in response to surgical injury and numerous pathologic conditions, including cancer and sepsis.[25] The observed higher concentration of Glu (and probably that of Asp as well) may reflect the energy demand at the luminal side of corneal/conjunctival epithelial cells. Mucosal tissue exhibits a high rate of aerobic glycolysis, and in intestinal metabolism, luminal Gln, Glu, and Asp, but not glucose, has been found to contribute critically to the respiratory CO_2 produced in this tissue.[26] Although considered nonessential, Gln becomes conditionally essential during severe catabolic stress in which intracellular and plasma Gln levels decrease rapidly.[27–29]

It is very difficult to discuss with clarity the underlying mechanism for the regulation of amino acid profiles in tear fluids, because to date, almost no information has been presented on the dynamic roles of ocular surface epithelial cells in regard to amino acid transportation. The presence of the Na^+-dependent neutral amino acid transporter has been reported in a rabbit primary corneal epithelial cell culture and rabbit corneas.[30] Whether all or part of the amino acid component of tear fluids is attributable to secretion, filtration, local synthesis, or local degradation of proteins is unknown. However, it is speculated that the amino acids are transported from tear fluids into the corneal tissues by this transport system. It is important to discuss the characteristic variance of amino acid profiles in tear fluid between the individuals with and without ocular surface disease. Diseases that develop because of the loss of corneal epithelial stem cells are known as limbal stem cell deficiency. Among limbal stem cell deficiency, SJS, ocular cicatricial pemphigoid, and severe chemical or thermal burns are known as severe ocular surface disease, because these diseases are intractable, even with corneal epithelial transplantation, and visual prognosis is poor. In cases of severe ocular surface disease, corneal neovascularization, ingrowth of fibrous tissue, and stromal scarring occur and often progress with chronic inflammation. However, the mechanisms of chronic inflammation and pathophysiology are still unclear. In this study, both the concentrations and relative composition of the amino acids differed between the severe ocular surface disease subjects and the non–ocular surface disease subjects. Hierarchical clustering on the amino acid profiles of tears clearly distinguished severe ocular surface disease subjects from non–ocular surface disease subjects. Surprisingly, hierarchical clustering also distinguished the eyes with SJS at the chronic stage as severe ocular surface disease, in which at least clinically, no inflammation and no scarring were detected. Amino acid profiles might be a sensitive marker of ocular surface inflammation, or they may be a new method to reflect ocular surface pathologic dynamics.

It is well known that supplemental Arg promotes wound healing following trauma shock. The major catabolic products of Arg are Orn and Cit. Because of the competition between nitric oxidase synthase and arginase for the same substrate Arg, their activities are regulated reciprocally. As for conditionally essential amino acids, Arg exhibited a significant decrease with a moderate decrease in Cit in the eyes with severe ocular surface disease, while Orn exhibited a prominent increase, indicating the possible polarization of tissue inflammation to the axis of arginase (oxidative tissue regeneration).[31–34] In this context, the reason why the increased composition of Orn over Cit, reflecting the high arginase activity, exists only in the tear fluids of individuals with chronic ocular surface inflammation is a subject that requires further investigation.

We can now harness information buried in amino acid profiles for the generation of diagnostic and surrogate markers. The methods described in this study might be applicable to the clinical setting and prove useful in diagnosing various physiologic and disease states at the ocular surface. Our results using cluster analysis of amino acid profiles in tear fluids suggest that the analysis can help us understand the complex interrelations that make up the metabolism of the ocular surface. In the future, a far more stringent study with controlled background factors will need to be performed to solidify the present observations. Amino acid represents a convenient set of metabolites that can be easily measured. Once the association of abnormalities in individual amino acid concentrations and/or composition with specific ocular surface diseases or physiologic conditions has been addressed, amino acid profiles for the generation of diagnostic and surrogate markers may prove to help advance biomedical and nutritional science in the field of ocular physiology.

PUBLICATION OF THIS ARTICLE WAS SUPPORTED IN PART BY HEALTH AND LABOR SCIENCES RESEARCH GRANTS (RESEARCH ON Intractable Diseases) from the Ministry of Health, Labour and Welfare of Japan, Tokyo, Japan, and the Japanese Ministry of Education, Culture, Sports, Science and Technology, Tokyo, Japan; a research grant from the Kyoto Foundation for the Promotion of Medical Science, Kyoto, Japan; and the Intramural Research Fund of Kyoto Prefectural University of Medicine, Kyoto, Japan. The authors indicate no financial conflict of interest. Involved in conception and design (C.S., J.H., S.K.); analysis and interpretation (M.N., C.S., K.S., N.O., H.M., J.H.); writing the article (M.N., C.S., A.O., J.H.); critical revision of the article (C.S., J.H., S.K.); final approval of the manuscript (M.N., C.S., K.S., N.O., H.M., A.O., J.H., S.K.); data collection (M.N., C.S.); provision of materials, patients, or resources (M.N., C.S.); statistical expertise (N.O., A.O.); obtaining funding (C.S., S.K.); and literature search (M.N., C.S., J.H.). All experimental procedures were approved by the Institutional Review Board for Human Studies at Kyoto Prefectural University of Medicine (KPUM). Prior informed consent was obtained from all patients, and this study was performed in accordance with the tenets of the Declaration of Helsinki for research involving human subjects.

REFERENCES

1. Holm E, Sedlaczek O, Grips E. Amino acid metabolism in liver disease. Curr Opin Clin Nutr Metab Care 1999;2(1): 47–53.
2. Hong SY, Yang DH, Chang SK. The relationship between plasma homocysteine and amino acid concentrations in patients with end-stage renal disease. J Ren Nutr 1998;8(1): 34–39.
3. Watanabe A, Higashi T, Sakata T, Nagashima H. Serum amino acid levels in patients with hepatocellular carcinoma. Cancer 1984;54(9):1875–1882.
4. Watanabe A, Takei N, Hayashi S, Nagashima H. Serum neutral amino acid concentrations in cirrhotic patients with impaired carbohydrate metabolism. Acta Med Okayama 1983;37(4):381–384.
5. Broer S. Amino acid transport across mammalian intestinal and renal epithelia. Physiol Rev 2008;88(1):249–286.
6. Fafournoux P, Bruhat A, Jousse C. Amino acid regulation of gene expression. Biochem J 2000;351(Pt 1):1–12.
7. Kilberg MS, Pan YX, Chen H, Leung-Pineda V. Nutritional control of gene expression: how mammalian cells respond to amino acid limitation. Annu Rev Nutr 2005;25:59–85.
8. van Sluijters DA, Dubbelhuis PF, Blommaart EF, Meijer AJ. Amino-acid-dependent signal transduction. Biochem J 2000; 351(Pt 3):545–550.
9. Wilmore DW. The effect of glutamine supplementation in patients following elective surgery and accidental injury. J Nutr 2001;131(9 Suppl):2543S–2549S; discussion 2550S–2551S.
10. Angele MK, Nitsch SM, Hatz RA, et al. L-arginine: a unique amino acid for improving depressed wound immune function following hemorrhage. Eur Surg Res 2002;34(1-2):53–60.
11. Nicklin P, Bergman P, Zhang B, et al. Bidirectional transport of amino acids regulates mTOR and autophagy. Cell 2009; 136(3):521–534.
12. Walker V, Mills GA. Quantitative methods for amino acid analysis in biological fluids. Ann Clin Biochem 1995;32(Pt 1):28–57.
13. Puck A, Liappis N, Hildenbrand G. Ion exchange column chromatographic investigation of free amino acids in tears of healthy adults. Ophthalmic Res 1984;16(5):284–288.
14. ChenZhuo L, Murube J, Latorre A, del Rio RM. Different concentrations of amino acids in tears of normal and human dry eyes. Adv Exp Med Biol 2002;506(Pt A):617–621.
15. Deyl Z, Hyanek J, Horakova M. Profiling of amino acids in body fluids and tissues by means of liquid chromatography. J Chromatogr 1986;379:177–250.
16. Shimbo K, Oonuki T, Yahashi A, Hirayama K, Miyano H. Precolumn derivatization reagents for high-speed analysis of amines and amino acids in biological fluid using liquid chromatography/electrospray ionization tandem mass spectrometry. Rapid Commun Mass Spectrom 2009;23(10): 1483–1492.
17. Iwatani S, Van Dien S, Shimbo K, et al. Determination of metabolic flux changes during fed-batch cultivation from measurements of intracellular amino acids by LC-MS/MS. J Biotechnol 2007;128(1):93–111.
18. Shimbo K, Yahashi A, Hirayama K, Nakazawa M, Miyano H. Multifunctional and highly sensitive precolumn reagents for amino acids in liquid chromatography/tandem mass spectrometry. Anal Chem 2009;81(13):5172–5179.
19. Noguchi Y, Zhang QW, Sugimoto T, et al. Network analysis of plasma and tissue amino acids and the generation of an amino index for potential diagnostic use. Am J Clin Nutr 2006;83(2):513S–519S.
20. Tom A, Nair KS. Assessment of branched-chain amino acid status and potential for biomarkers. J Nutr 2006;136(1 Suppl):324S–330S.
21. Cynober LA. Plasma amino acid levels with a note on membrane transport: characteristics, regulation, and metabolic significance. Nutrition 2002;18(9):761–766.
22. Redmond HP, Stapleton PP, Neary P, Bouchier-Hayes D. Immunonutrition: the role of taurine. Nutrition 1998;14(7–8): 599–604.
23. Pasantes-Morales H, Wright CE, Gaull GE. Taurine protection of lymphoblastoid cells from iron-ascorbate induced damage. Biochem Pharmacol 1985;34(12):2205–2207.
24. Skrovanek S, Valenzano MC, Mullin JM. Restriction of sulfur-containing amino acids alters claudin composition and improves tight junction barrier function. Am J Physiol Regul Integr Comp Physiol 2007;293(3):R1046–1055.
25. Stapleton PP, O'Flaherty L, Redmond HP, Bouchier-Hayes DJ. Host defense—a role for the amino acid taurine? JPEN J Parenter Enteral Nutr 1998;22(1):42–48.
26. Windmueller HG, Spaeth AE. Respiratory fuels and nitrogen metabolism in vivo in small intestine of fed rats. Quantitative importance of glutamine, glutamate, and aspartate. J Biol Chem 1980;255(1):107–112.
27. Sakiyama T, Musch MW, Ropeleski MJ, Tsubouchi H, Chang EB. Glutamine increases autophagy under basal and stressed conditions in intestinal epithelial cells. Gastroenterology 2009;136(3):924–932.
28. Askanazi J, Carpentier YA, Michelsen CB, et al. Muscle and plasma amino acids following injury. Influence of intercurrent infection. Ann Surg 1980;192(1):78–85.
29. Parry-Billings M, Evans J, Calder PC, Newsholme EA. Does glutamine contribute to immunosuppression after major burns? Lancet 1990;336(8714):523–525.
30. Katragadda S, Talluri RS, Pal D, Mitra AK. Identification and characterization of a Na+-dependent neutral amino acid transporter, ASCT1, in rabbit corneal epithelial cell culture and rabbit cornea. Curr Eye Res 2005;30(11):989–1002.
31. Murata Y, Amao M, Hamuro J. Sequential conversion of the redox status of macrophages dictates the pathological progression of autoimmune diabetes. Eur J Immunol 2003;33(4): 1001–1011.
32. Murata Y, Yamashita A, Saito T, Sugamura K, Hamuro J. The conversion of redox status of peritoneal macrophages during pathological progression of spontaneous inflammatory bowel disease in Janus family tyrosine kinase 3(-/-) and IL-2 receptor gamma(-/-) mice. Int Immunol 2002;14(6):627–636.
33. Gordon S, Taylor PR. Monocyte and macrophage heterogeneity. Nat Rev Immunol 2005;5(12):953–964.
34. Mosser DM, Edwards JP. Exploring the full spectrum of macrophage activation. Nat Rev Immunol 2008;8(12):958–969.

Biosketch

Mina Nakatsukasa, MD, graduated and received her medical degree from Kyoto Prefectural University of Medicine, Kyoto, Japan in 2001, and completed her residency training at the Department of Ophthalmology at Kyoto Prefectural University Hospital, Kyoto, Japan. Dr Nakatsukasa currently specializes in clinical research and cornea-related diseases.

The Application of In Vivo Confocal Scanning Laser Microscopy in the Diagnosis and Evaluation of Treatment Responses in Mooren's Ulcer

Shin Hatou,[1] *Murat Dogru,*[2] *Osama M. A. Ibrahim,*[1,2] *Tais Wakamatsu,*[1,2] *Enrique Adan Sato,*[2] *Shigeto Shimmura,*[1] *Kazuno Negishi,*[1] *and Kazuo Tsubota*[1]

Purpose. To evaluate the extent of corneal inflammation and the response to treatment in patients with Mooren's ulcer, by in vivo confocal microscopy (IVCM).

Methods. Twenty-two eyes of 15 patients with Mooren's ulcer were enrolled in this prospective study. All subjects underwent routine ophthalmic examinations, IVCM, and conjunctival histopathologic examination of specimens in patients undergoing conjunctival excision. Eyes with active ulcer were treated with topical corticosteroids and additional therapy, depending on the signs and symptoms. Eyes in remission continued to receive the previous treatment protocols. The relation between the severity of ulcer and inflammation status as assessed by IVCM was also studied. The endpoints were inflammatory cell density (ICD), counted by IVCM, and the extent of the limbal arc involved with ulcers.

Results. Ten eyes had active corneal ulcers, and 12 eyes had been in remission for the past year. The mean ICD of eyes with active ulcers before treatment was 2092.7 ± 1538.6 cells/mm^2 (range, 835.3–7832.7; 95% CI, 3232.5–952.9). Nine of the eyes improved at 8 weeks, with a decrease in ICD to 249.1 ± 109.0 cells/mm^2 (range, 100.3–595.3; 95% CI, 329.8–168.3). One eye had corneal perforation, and ICD immediately before perforation was 1677.6 ± 247.6 cells/mm^2. The mean ICD of 12 eyes in remission was 357.5 ± 266.8 cells/mm^2 (range, 12.7–1127.0; 95% CI, 555.2–159.8). The correlation of the ICD and the extent of limbal involvement with ulcers was strong (R^2 = 0.8119).

Conclusions. ICD evaluated by IVCM is a useful and promising parameter for evaluation of the degree of inflammation in eyes with Mooren's ulcer and for assessment of response to treatment. (*Invest Ophthalmol Vis Sci.* 2011;52:6680–6689) DOI:10.1167/iovs.10-5906

Mooren's ulcer begins as a crescent-shaped gray-white infiltrate in the peripheral cornea, which usually progresses to epithelial breakdown and stromal melting, eventually developing into a chronic, usually painful, peripheral corneal ulcer.[1] The leading edges of the ulcer are undermined, infiltrated, and deepithelialized, and the adjacent conjunctiva and sclera are usually inflamed and hyperemic.[1] Histopathology of resected conjunctiva from subjects with Mooren's ulcer has been reported to show a large number of plasma cells, lymphocytes, and histiocytes.[2]

Currently, a stepladder approach to therapy is recommended.[3] Initially, patients with Mooren's ulcer are aggressively treated with topical corticosteroids.[3] If there is no improvement in the signs and symptoms, conjunctival excision is performed. Systemic immunosuppressive agents (prednisolone, cyclosporine, cyclophosphamide, methotrexate, or azathioprine) can be used.[3–6] If such management steps fail or there is a corneal perforation or descemetocele, surgical approaches such as amniotic membrane transplants, keratoepithelioplasty, or lamellar or penetrating keratoplasty can be performed.[6–10]

The response to therapy is generally judged subjectively by degree of pain and the conventional slit lamp microscopic examination, such as resolution of conjunctival hyperemia, ciliary injection, and corneal reepithelization judged by fluorescein staining.[3] It is important to quantify the degree of inflammation and the changes in response to treatment in patients with Mooren's ulcer. In vivo laser scanning confocal microscopy is a new emerging less-invasive technology, which is useful as a supplementary diagnostic tool for in vivo assessment of the histopathology of many ocular surface diseases and anterior segment disorders.[11–18] In this study, we used in vivo laser scanning confocal microscopy (the Rostock Corneal Software Version 1.2 of the Heidelberg Retina Tomograph II: RCM/HRT II; Heidelberg Engineering, Dossenheim, Germany) to evaluate the degree of inflammation in the cornea and conjunctiva of patients with Mooren's ulcer and also to study the changes in response to anti-inflammatory treatment. To the best of our knowledge, this is the first report to describe the confocal laser microscopy findings in Mooren's ulcer.

Materials and Methods

Fifteen adult patients (seven men, eight women; mean age, 59.9 ± 19.4 years) with a diagnosis of Mooren's ulcer who were willing to comply with the protocol and who provided informed consent were enrolled in the study. Examination procedures were board reviewed. The study complied with the principles of the Declaration of Helsinki for research involving human subjects. Ten eyes of seven patients who had active peripheral corneal ulcers in the peripheral cornea, with pain and the adjacent inflamed and hyperemic conjunctiva and sclera, were diagnosed as patients with active Mooren's ulcer. Twelve eyes of nine patients with a history of Mooren's ulcer, whose corneal ulcers had not relapsed for the past 12 months, were diagnosed as Mooren's ulcers in remission. One patient had bilateral

From the [1]Department of Ophthalmology, Keio University School of Medicine, Tokyo, Japan; and [2]Johnson & Johnson Ocular Surface and Visual Optics Department, Keio University School of Medicine, Tokyo, Japan.

Supported by a grant from the Japanese Ministry of Health, Labor, and Welfare. The funding organization had no role in the design or conduct of the research.

Submitted for publication May 19, 2010; revised November 5, 2010, and April 9, 2011; accepted May 27, 2011.

Disclosure: **S. Hatou**, None; **M. Dogru**, None; **O.M.A. Ibrahim**, None; **T. Wakamatsu**, None; **E.A. Sato**, None; **S. Shimmura**, None; **K. Negishi**, None; **K. Tsubota**, None

Corresponding author: Shin Hatou, Department of Ophthalmology, Keio University School of Medicine, 35 Shinanomachi, Shinjuku, Tokyo 160-8582, Japan; tr97469@zc4.so-net.ne.jp.

Mooren's ulcers, whose right eye was in remission and whose left eye was active. Patients who had rheumatoid arthritis or other collagen vascular diseases, staphylococcal marginal keratitis accompanied by blepharitis, infectious ulcers, giant cell arteritis, local infectious causes, including herpes simplex and herpes zoster, Terrien's degeneration, pellucid marginal degeneration, senile furrow degeneration, ocular rosacea, or leukemia, were excluded.[6] To exclude rheumatoid arthritis and other collagen diseases, blood tests of RA factor, antinuclear antibody, anti-Ro/SSA antibody, anti-La/SSB antibody, CRP, and CBC were performed. To exclude staphylococcal marginal keratitis or other infectious diseases, we performed bacterial cultures from conjunctival sac swabs, eye discharge, or margin of ulcers. To exclude herpes simplex and herpes zoster infections, we requested SRL Laboratory (Tokyo, Japan) to perform herpes antigen test by the fluorescein antibody (FA) method using scratch samples from the ulcer beds. Other diseases meeting the exclusion criteria were checked by clinical record and anamnesis.

Patients with active Mooren's ulcers underwent in vivo laser confocal microscopy and a complete ophthalmic examination, including measurement of visual acuity and intraocular pressure, slit lamp microscopic examination, and dilated fundus examination at the enrollment visit, day 0. At the study follow-up visits (scheduled on weeks 1, 4, and 8 after enrollment), in vivo laser confocal microscopy and ophthalmic examination were performed, consisting of visual acuity testing, intraocular pressure, and slit lamp microscopic examination. At the enrollment visit, patients with Mooren's ulcers in remission underwent in vivo laser confocal microscopy and ophthalmic examination, including slit lamp microscopic examination.

All patients at day 0 had anterior segment photographs and slit lamp microscopic examination, including fluorescein staining of the ocular surface. The extent of limbal involvement with ulcers and adjacent gray-white infiltration was expressed in degrees (0-360°). To measure it, the corneal circumference of a slit lamp photograph was divided in 24 sections of 15° each. The count of sections of limbal involvement along with ulcers was then recalculated in degrees. The extent of limbal involvement in eyes with Mooren's ulcer in remission was regarded as 0°, according to the protocol of the study.

In vivo laser confocal scanning laser microscopy (CSLM) was performed on all subjects with a new-generation confocal microscope (the Rostock Corneal Software, ver. 1.2, Heidelberg Retina Tomograph II [RCM/HRT II]; Heidelberg Engineering GmbH). After the administration of topical anesthesia with 0.4% oxybuprocaine, the subject's chin was placed in the chin rest. The objective of the microscope was an immersion lens (magnification 63×; Carl Zeiss, Oberkochen, Germany) covered by a polymethylmethacrylate (PMMA) cap (Tomo-cap; Heidelberg Engineering GmbH). Comfort gel (Bausch & Lomb, GmbH, Berlin, Germany) was used as a coupling agent between the applanating lens cap and the conjunctiva. By adjusting the controller, the center of the cap was applanated onto the cornea, and in vivo digital images of the cornea were visualized directly on the computer screen. When the first superficial cells were seen, the digital micrometer gauge was set at 0; then, when the operator pressed on the foot pedal, sequence images were recorded by a charge-coupled device (CCD) color camera (maximum 30 frames/s) while the focal plane was gradually moved forward into the corneal stroma. Corneal and adjacent limbal conjunctival lesions were scanned while the applanating lens was moved through the entire length of the ulcer with minute vertical or horizontal movements. Four nonoverlapping areas with images of inflammatory cells were selected from all vertical scan areas, and inflammatory cell density (ICD) was counted at the basal cell layer level of the corneal epithelium in each 400 × 400-μm frame, with the help of the accompanying software. To avoid overlap, the scans were performed along the entire length of the ulcers on the limbal side, central corneal side, and superior/inferior edges, at all four sites with minute movements of the PMMA cap, and three nonoverlapping scans per site with best resolution quality were selected and underwent ICD calculations. The depth chosen for ICD calculations in the ulcers corresponded to the level of the healthy basal epithelium along the edge of the ulcer. White round cells of 5- to 15-μm diameter were chosen for counting ICD, and images with many dendritic cells were not used, because it is hard to count dendritic cells accurately. The mean ICD of each (limbal side, central side, superior edge, and inferior edge) site and the mean of ICDs of the four sites was calculated. Confocal microscopy scans were performed by one examiner who was masked to the diagnosis of the subjects. Analysis of the scans was performed by three different investigators who were also masked to the diagnosis in each case. For intraobserver variability testing, the same investigator performed the same ICD analysis on three occasions. For evaluating intraobserver variability, these investigators carried out ICD calculations, and the differences between the investigator calculations were sought.

The laser source used in the Retina Tomograph II/Rostock Corneal Module (Heidelberg Engineering) is a diode laser with a wavelength of 670 nm. Two-dimensional images consisted of 384 × 384 picture elements, covering an area of 400 × 400-μm field of the view (FOV). The transverse field of view was captured with the 400 FOV lens. Digital resolution was quoted as 1 μm/pixel transversely and 2 μm/pixel longitudinally by the manufacturer.

Eyes with active Mooren's ulcer were treated with topical corticosteroids and additional therapy, including systemic corticosteroids, topical cyclosporine, systemic cyclosporine, conjunctival excision, and/or keratoepithelioplasty in a severity-based stepladder approach.[1] Eyes with Mooren's ulcer in remission continued to receive the previous treatment protocols.

Statistical Analysis

Data are presented as the mean ± SD and were compared by Student's *t*-test or Kruskal-Wallis test. Correlations were analyzed by Pearson's correlation analysis (Excel 2007 software; Microsoft, Redmond, WA). $P < 0.05$ denoted statistical significance.

Results

Patient Characteristics

Ten eyes had active ulcers, and 12 eyes were in remission. The patients' characteristics, extent of limbal involvement with ulcers in degrees of arc (deg arc), and the mean ICDs calculated from in vivo confocal microscopic images are shown in Table 1. The intraobserver variability of the ICD measurement was 14.3 ± 17.3 (maximum, 54.7; minimum, 0) cells/mm^2 and interobserver variability was 58.0 ± 62.9 (maximum, 146.7; minimum, 2.7) cells/mm^2. The left eye of patient 1 could not be examined by in vivo confocal microscopy at day 0, due to refusal by the patient. The mean ICD in the nine eyes with active ulcers before treatment was 2092.7 ± 1538.6 cells/mm^2 (range, 835.3-7832.7; 95% CI, 3232.5-952.9). The mean ICD in the 12 eyes in remission was 357.5 ± 266.8 cells/mm^2 (range, 12.7-1127.0; 95% CI, 555.2-159.8). To demonstrate that there was an adequate number of eyes for a more than 80% power, one-sided analysis was performed with the following calculation:

$$n \geq \sigma^2(Z\alpha + Z\gamma)^2/(\mu - \mu_0)^2 = 4.87$$

where n is the number, σ is the standard deviation, $Z\alpha$ is the percentage of the 0.05 significance level = 1.64; $Z\gamma$ is the percentage of the 0.20 significance level = 0.84; μ is the expected (i.e., mean value) ICD in the eyes with active ulcers, and μ_0 is the expected ICD in the eyes in remission.

An adequate number was more than 4.87, and the number of recruited eyes with active ulcer exceeded the adequate number.

The treatment outcome and ICD decrease/week in 10 eyes with active ulcers are shown in Table 2A. All 10 eyes with active ulcers were treated initially with hourly topical betamethasone eyedrops. In addition, 9 of 10 subjects received topical cyclosporine three times a day. Five of these 10 subjects received additional

Table 1. Patients' Characteristics and Examination Findings

A. Active Ulcers

Patient	Eye No.	Age	Sex	Eye R/L	Extent of Limbal Involvement with Ulcers (deg arc)	Confocal Microscopy					Limbal Subconjunctival Cysts Harboring Polymorphs
							ICD (cells/mm^2)				
							Day 0	1 Week	4 Weeks	8 Weeks	
Patient 1	1	36	M	R	360	Limbal	7832.7 ± 548.3	1069.3 ± 158.1	844.3 ± 424.1	595.3 ± 514.3	
						Central	2975.7 ± 1114.8	647.0 ± 468.8	766.7 ± 523.4	380.0 ± 53.4	
						Superior	4721.3 ± 2850.8	846.7 ± 476.1	857.0 ± 351.9	506.3 ± 369.4	(+)
						Inferior	3490.0 ± 1521.9	751.3 ± 600.2	421.7 ± 247.2	449.0 ± 105.7	
						Mean	5524.4 ± 2526.0	828.6 ± 421.6	722.4 ± 387.7	482.7 ± 286.8	
	2			L	360		Not examined	Not examined	Not examined	Not examined	
Patient 2	3	51	F	L	150	Limbal	2319.7 ± 948.5	1428.3 ± 535.6	380.3 ± 353.1	233.0 ± 102.7	
						Central	1575.7 ± 478.8	791.7 ± 582.7	35.3 ± 37.8	260.0 ± 84.3	
						Superior	1601.0 ± 539.4	1156.7 ± 750.7	180.0 ± 176.0	126.0 ± 6.0	(+)
						Inferior	1429.0 ± 289.3	1015.3 ± 431.0	178.3 ± 217.2	164.3 ± 57.7	
						Mean	1731.3 ± 635.5	1098.0 ± 555.2	193.5 ± 231.5	195.8 ± 83.2	
Patient 3	4	92	F	L	90	Limbal	1935.0 ± 224.2	440.3 ± 203.8	406.3 ± 226.6	394.0 ± 291.5	
						Central	1329.3 ± 765.5	169.0 ± 173.9	287.0 ± 65.0	234.0 ± 240.8	
						Superior	1971.7 ± 258.5	322.7 ± 224.4	281.7 ± 136.7	273.3 ± 313.7	(+)
						Inferior	1256.3 ± 351.6	245.7 ± 211.9	260.0 ± 153.0	141.7 ± 79.6	
						Mean	1623.1 ± 519.8	294.4 ± 203.3	308.8 ± 146.1	260.8 ± 232.4	
Patient 4	5	62	F	L	120	Limbal	1839.7 ± 180.5	1846.0 ± 315.5	938.3 ± 181.4	131.7 ± 85.2	
						Central	1505.3 ± 417.1	1569.3 ± 158.9	448.0 ± 286.0	271.3 ± 134.2	(+), (fluid-filled cyst(+) before perforation)
						Superior	1667.7 ± 553.3	1556.0 ± 100.3	765.0 ± 294.5	107.7 ± 26.8	
						Inferior	1551.3 ± 463.1	1739.0 ± 338.2	506.3 ± 421.6	100.3 ± 45.3	
						Mean	1641.0 ± 387.8	1677.6 ± 247.6	664.4 ± 334.3	152.8 ± 101.8	
Patient 5	6	69	F	L	60	Limbal	2114.7 ± 158.1	1810.3 ± 550.5	675.3 ± 402.9	255.3 ± 169.8	(+)
						Central	1627.3 ± 327.8	1470.7 ± 368.5	771.0 ± 202.7	303.7 ± 171.9	
						Superior	1839.7 ± 828.3	1308.0 ± 500.7	926.3 ± 498.5	176.3 ± 73.5	
						Inferior	1793.7 ± 460.2	1358.0 ± 440.6	445.7 ± 266.6	208.0 ± 124.2	
						Mean	1843.8 ± 469.9	1486.8 ± 450.0	704.6 ± 358.1	235.8 ± 130.1	
Patient 6	7	30	F	R	30	Limbal	1301.3 ± 243.5	1078.3 ± 347.0	676.7 ± 181.6	145.0 ± 37.3	
						Central	835.3 ± 182.8	453.7 ± 348.5	386.0 ± 76.3	132.3 ± 61.7	
						Superior	1082.0 ± 566.0	753.3 ± 285.5	315.7 ± 39.6	218.7 ± 265.6	(−)
						Inferior	1143.0 ± 492.5	352.3 ± 223.8	234.3 ± 100.7	250.7 ± 248.8	
						Mean	1090.4 ± 387.1	659.4 ± 394.3	403.2 ± 198.8	186.7 ± 166.4	
	8	30	F	L	45	Limbal	1455.3 ± 48.6	1099.0 ± 336.0	558.3 ± 762.2	322.0 ± 185.5	
						Central	1150.7 ± 486.0	635.3 ± 309.9	118.0 ± 16.5	157.3 ± 110.4	
						Superior	987.7 ± 79.0	654.3 ± 357.0	145.7 ± 75.4	202.3 ± 117.7	(−)
						Inferior	1185.7 ± 194.6	302.7 ± 198.2	139.3 ± 114.5	234.3 ± 128.5	
						Mean	1194.8 ± 286.6	672.8 ± 394.6	240.3 ± 382.1	229.0 ± 134.0	

(*continues*)

TABLE 1 (*continued*). Patients' Characteristics and Examination Findings

Patient	Eye No.	Age	Sex	Eye R/L	Extent of Limbal Involvement with Ulcers (deg arc)	Confocal Microscopy					
						ICD (cells/mm²)					Limbal Subconjunctival Cysts Harboring Polymorphs
							Day 0	1 Week	4 Weeks	8 Weeks	
Patient 7	9	34	M	R	360	Limbal	4564.7 ± 1127.5				
						Central	2950.7 ± 1017.1				
						Superior	2603.7 ± 1757.2	Not examined	Not examined	Not examined	(+)
						Inferior	3446.3 ± 1391.5				
						Mean	3391.3 ± 1389.7				
	10		M	L	360	Limbal	2621.7 ± 1321.6				
						Central	2775.0 ± 1759.1				
						Superior	2489.7 ± 1083.4	Not examined	Not examined	Not examined	(+)
						Inferior	2549.0 ± 578.7				
						Mean	2608.8 ± 1080.2				
Overall mean ± SD (1–8)*						2092.7 ± 1538.9	969.7 ± 490.7	462.5 ± 229.4	249.1 ± 109.0		
(95% CI)							(3232.5–952.9)	(1323.1–596.2)	(632.4–292.5)	(329.8, 168.3)	

B. Ulcers In Remission

Patient	Eye No.	Age	Sex	Eye (R/L)	Extent of Limbal Involvement with Ulcers (deg arc)	Confocal Microscopy		
							ICD (cells/Mm²)	Limbal Subconjunctival Cysts Harboring Polymorphs
Patient 2	11	51	F	L	0	Limbal	12.7 ± 2.5	
						Central	25.0 ± 5.6	
						Superior	41.3 ± 6.5	(−)
						Inferior	25.3 ± 9.0	
						Mean	26.1 ± 11.9	
	12			R	0	Limbal	173.0 ± 70.2	
						Central	121.0 ± 107.0	
						Superior	725.3 ± 74.5	(−)
						Inferior	337.7 ± 92.0	
						Mean	339.3 ± 258.3	
Patient 8	13	71	M	L	0	Limbal	118.7 ± 59.0	
						Central	450.7 ± 88.5	
						Superior	123.7 ± 25.0	(−)
						Inferior	221.0 ± 57.1	
						Mean	228.5 ± 150.1	
Patient 9	14	77	M	L	0	Limbal	890.0 ± 76.2	
						Central	669.7 ± 203.9	
						Superior	673.0 ± 51.7	(−)
						Inferior	575.7 ± 125.2	
						Mean	702.1 ± 162.7	

(*continues*)

TABLE 1 (*continued*). Patients' Characteristics and Examination Findings

Patient	Eye No.	Age	Sex	Eye (R/L)	Extent of Limbal Involvement with Ulcers (deg arc)	Confocal Microscopy		
							ICD (cells/Mm^2)	Limbal Subconjunctival Cysts Harboring Polymorphs
Patient 10	15	54	M	R	0	Limbal	133.0 ± 33.0	
						Central	172.0 ± 22.6	
						Superior	191.3 ± 54.3	(−)
						Inferior	167.7 ± 72.4	
						Mean	166.0 ± 47.6	
	16			L	0	Limbal	735.3 ± 351.7	
						Central	638.3 ± 157.9	
						Superior	666.0 ± 221.6	(−)
						Inferior	671.7 ± 198.4	
						Mean	677.8 ± 210.9	
Patient 11	17	57	F	R	0	Limbal	773.7 ± 195.0	(−)
						Central	1127.0 ± 218.8	
						Superior	778.3 ± 78.4	
						Inferior	641.7 ± 313.3	
						Mean	830.2 ± 264.4	
	18			R	0	Limbal	226.3 ± 112.2	
						Central	86.0 ± 32.1	
						Superior	69.7 ± 30.9	(−)
						Inferior	106.3 ± 41.5	
						Mean	122.1 ± 84.3	
Patient 12	19	88	M	L	0	Limbal	48.0 ± 13.0	
						Central	195.3 ± 29.6	
						Superior	146.3 ± 12.5	(−)
						Inferior	160.3 ± 45.2	
						Mean	137.5 ± 62.1	
Patient 13	20	41	M	L	0	Limbal	586.7 ± 149.5	
						Central	151.7 ± 24.0	
						Superior	235.7 ± 105.9	(−)
						Inferior	199.7 ± 65.9	
						Mean	293.4 ± 198.1	
Patient 14	21	59	F	R	0	Limbal	186.7 ± 92.8	
						Central	343.3 ± 46.5	
						Superior	130.7 ± 7.0	(−)
						Inferior	148.0 ± 49.9	
						Mean	202.2 ± 100.6	
Patient 15	22	78	F	R	0	Limbal	483.0 ± 219.2	
						Central	649.0 ± 367.2	
						Superior	645.7 ± 89.2	(−)
						Inferior	481.7 ± 168.5	
						Mean	564.8 ± 217.5	
Overall Mean ± SD (95% CI)							357.5 ± 266.8 (555.2–159.8)	

The patients' characteristics, extent of limbal ulcer involvement in degrees of arc (0–360°), appearance of limbal subconjunctival cysts harboring polymorphs, and ICDs of the limbal side, central side, superior edge, inferior edge, and mean of these four sites, calculated from in vivo confocal microscopy images. (A) Patients with active Mooren's ulcers. (B) Patients with Mooren's ulcers in remission. Eyes 9 and 10 were excluded from the calculation of mean ICD (A) because patient 7 was lost to follow-up. If these eyes were included, the mean ICD ± SD would be 2294.3 ± 1404.9 cells/mm^2 and the 95% CI, 3335.1–1253.6.

TABLE 2. Treatment and Course of Patients

A. Active Ulcers

Patient	Eye No.	Treatment	Course	ICD Decrease (cells/mm^2/wk)
Patient 1	1	Topical betamethasone/topical cyclosporine/systemic	Improved	4695.8
	2	Methylprednisolone/systemic cyclosporine	Improved	—
Patient 2	3	Topical betamethasone/topical cyclosporine	Improved	633.3
Patient 3	4	Topical betamethasone	Improved	1328.7
Patient 4	5	Topical betamethasone/topical cyclosporine after the corneal perforation conjunctival excision and keratoepithelioplasty/ systemic-cyclosporine/systemic prednisolone	Corneal perforation, 8 days after initiation of treatment	−36.6
Patient 5	6	Topical betamethasone/topical cyclosporine/conjunctival excision	Improved	357.1
Patient 6	7	Topical betamethasone/topical cyclosporine	Improved	431.0
	8	Topical betamethasone/topical cyclosporine	Improved	522.0
Patient 7	9	Topical betamethasone/topical cyclosporine/systemic prednisolone	Lost to follow-up	—
	10			—
			Mean ± SD	1447.6 ± 1985.7

B. Ulcers In Remission

Patient	Eye No.	Treatment	Periods in Remission
Patient 2	11	Free of therapy	2 Years and 2 months
Patient 8	12	Topical betamethasone	1 Year 1 month
	13	Topical betamethasone	1 Year 1 month
Patient 9	14	Topical betamethasone	3 Years 4 months
Patient 10	15	Topical betamethasone	3 Years
	16	Topical betamethasone	3 Years
Patient 11	17	Topical betamethasone	10 Years
Patient 12	18	Topical betamethasone	2 Years and 3 months
	19	Topical betamethasone	2 Years 3 months
Patient 13	20	Topical betamethasone	1 Year
Patient 14	21	Topical betamethasone	1 Year 1 month
Patient 15	22	Topical betamethasone	1 Year

The treatment outcome of patients with active Mooren's ulcers (A), and treatment and periods in remission of patients with Mooren's ulcers in remission, (B). ICD decrease per week of patients with active Mooren's ulcers are also expressed.

systemic corticosteroids; 3 of the 10 received systemic cyclosporine. Seven of the eyes responded to subsequent treatment at 8 weeks with improvement in conjunctival injection and corneal re-epithelization. Eyes 9 and 10 of patient 7 were lost to follow-up. The mean ICD decrease per week in the seven eyes with active ulcers was 1109.2 ± 1644.7 cells/mm^2/wk. ICD decrease per week of treatment was observed to be less in the patient with corneal perforation and the patient who did not respond to treatment and underwent conjunctival excision. The treatment and periods in remission of the eyes in remission are shown in Table 2B. Eleven of the 12 eyes in remission were treated with topical betamethasone three to six times a day, and one eye received no therapy. Pearson's correlation analysis revealed that the correlation between ICD and periods of remission was not significant ($P = 0.086$; $R^2 = 0.2663$).

The anterior segment photographs, fluorescein staining of the ocular surface, and in vivo laser confocal microscopy findings of the left eye of patient 2 are shown in Figure 1. The patient had already relapsed several times, and vessels as well as conjunctival invasion were seen in the superior corneal limbus (Fig. 1A). The corneal ulcer relapsed at the head of the conjunctival invasion (Figs. 1A, 1B). In vivo confocal microscopy scans of four sites (limbal side, central side, superior edge, and inferior edge) disclosed marked infiltration with dendritic cells as well as polymorphs (Figs. 1C-1-1C-4,). Dark cysts harboring numerous polymorphs were also seen in limbal subconjunctival regions (Fig. 1D, 1E). Such cysts were seen in six of seven patients with active ulcers, but were exclusively nonobservable in all eyes in remission (Table 1). Although the corneal ulcers of patient 2 extended up to 150°, the ulcer was shallow and responded to the treatment very well (Figs. 1F, 1G), and the ICD of each site immediately decreased with subsequent treatment (Figs. 1H-1-1H-4).

The left eye of patient 4 had a corneal perforation 8 days after initiation of treatment (Fig. 2A). In vivo confocal microscopy scans disclosed marked infiltration by inflammatory cells (Figs. 2B-1-2B-4), with a mean ICD immediately before perforation of 1677.6 ± 247.6 cells/mm^2. The scan also revealed marked infiltration with inflammatory cells in the corneal epithelial basal cell area, as well as cysts filled with inflammatory infiltrates and fluid-filled cysts in the limbal subconjunctival region (Figs. 2C, 2D). Conjunctival excision and keratoepithelioplasty were performed, and, after the operation, the ulcer healed and the patient was free of relapses. The corresponding area in histopathology specimens and ex vivo confocal microscopy examinations showed similar anatomic details and findings including polymorphs, and subconjunctival cysts (Figs. 2E, 2F). These findings reflected polymorphs and cysts seen in Figures 2C and 2D.

Correlation between ICD and the Extent of Mooren's Ulcer

Pearson's correlation analysis revealed that the correlation of the mean ICD or ICD in each site at the enrollment visit was

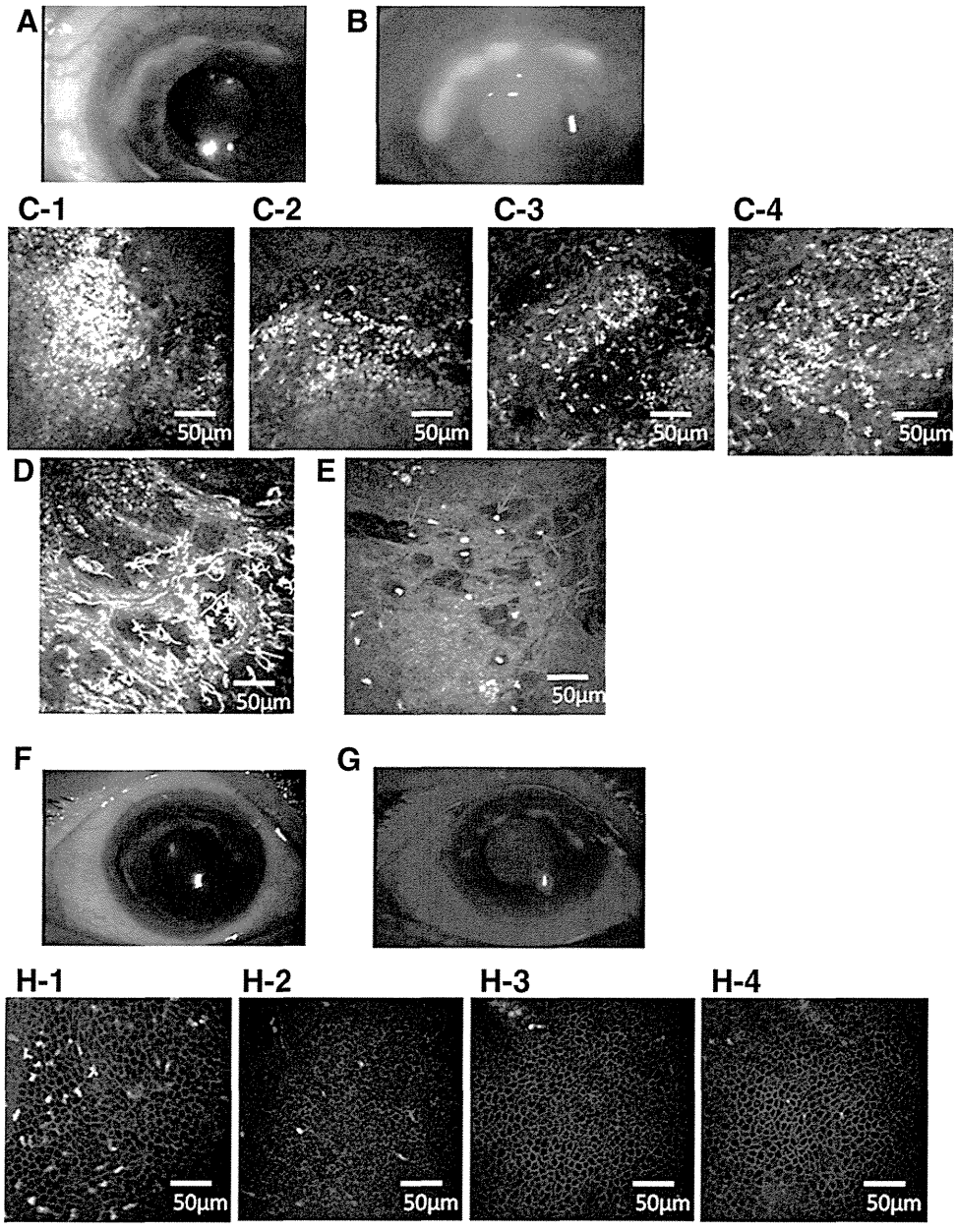

FIGURE 1. Slit lamp microscopy examination, fluorescein staining of the ocular surface, and in vivo laser confocal microscopy findings in the left eye of patient 2. (**A**, **B**) Slit lamp photograph and fluorescein staining at the enrollment day. (**C**) In vivo confocal microscopy scan showing marked infiltration with polymorphs, which were counted to determine the ICD (**C-1**; limbal side, **C-2**; central side, **C-3**; superior edge, **C-4**; inferior edge). (**D**) Dendritic cells (*yellow arrows*) were also seen. (**E**) Dark cysts harboring polymorphs in the limbal subconjunctival region (*red arrows*). (**F**, **G**) In response the treatment, epithelization improved and the corneal ulcers regressed in 1 week. (**H**) In vivo confocal microscopy scans of limbal side (**H-1**), central side (**H-2**), superior edge (**H-3**), and inferior edge (**H-4**) in 1 week. Note that the infiltration decreased substantially.

very strong and the limbal involvement with ulcers measured by slit lamp microscopic examination was extensive (limbal side: R^2=0.7618, $P = 1.8726 \times 10^{-7}$; central side, R^2=0.8775, $P = 1.213 \times 10^{-8}$; superior edge; R^2=0.7798, $P = 1.150 \times 10^{-6}$, inferior edge; R^2=0.8832, $P = 2.747 \times 10^{-8}$, mean of four sites; $R^2 = 0.8199$, $P = 2.256 \times 10^{-8}$; Fig. 3).

ICD Alterations with Treatment

The change of mean ICD in eyes with active Mooren's ulcers in response to treatment is shown in Figure 4. Eyes 9 and 10 of patient 7 were excluded in this figure because the patient was lost to follow-up. At enrollment day, the mean ICD of the limbal side was the highest (2685.5 ± 2297.1) and the mean ICD of the central side was lowest (1571.3 ± 677.8) among the four sites. The Kruskal-Wallis test revealed no significant difference between the ICDs of these four sites. The ICD of each site in eyes with active Mooren's ulcers gradually decreased to the same level as that of eyes in remission with response to subsequent treatment. There was a significant decrease in the mean ICD at 1 month (462.5 ± 229.4 cells/mm^2; range, 35.3-938.3; 95% CI, 632.4-292.5) and 2 months (249.1 ± 109.0 cells/mm^2; range, 100.3-595.3; 95% CI, 329.8-168.3) of treatment, compared with the baseline (day 0) values. The mean ICD in patients with active Mooren's ulcers was also significantly higher than that in eyes of patients with Mooren's ulcers in remission (357.5 ± 266.8 cells/mm^2; range, 12.7-1127.0; 95% CI, 555.2-159.8).

DISCUSSION

Mooren's ulcer is an autoimmune corneal disease of unknown etiology.[1] The diagnosis of Mooren's ulcer is a diagnosis of exclusion requiring an extensive search for a wide variety of diseases causing peripheral ulcerative keratitis, including rheumatoid arthritis and other collagen vascular diseases, staphylococcal marginal keratitis accompanied by blepharitis, giant cell arteritis, local infectious causes including herpes simplex and herpes zoster, Terrien's degeneration, pellucid marginal degen-

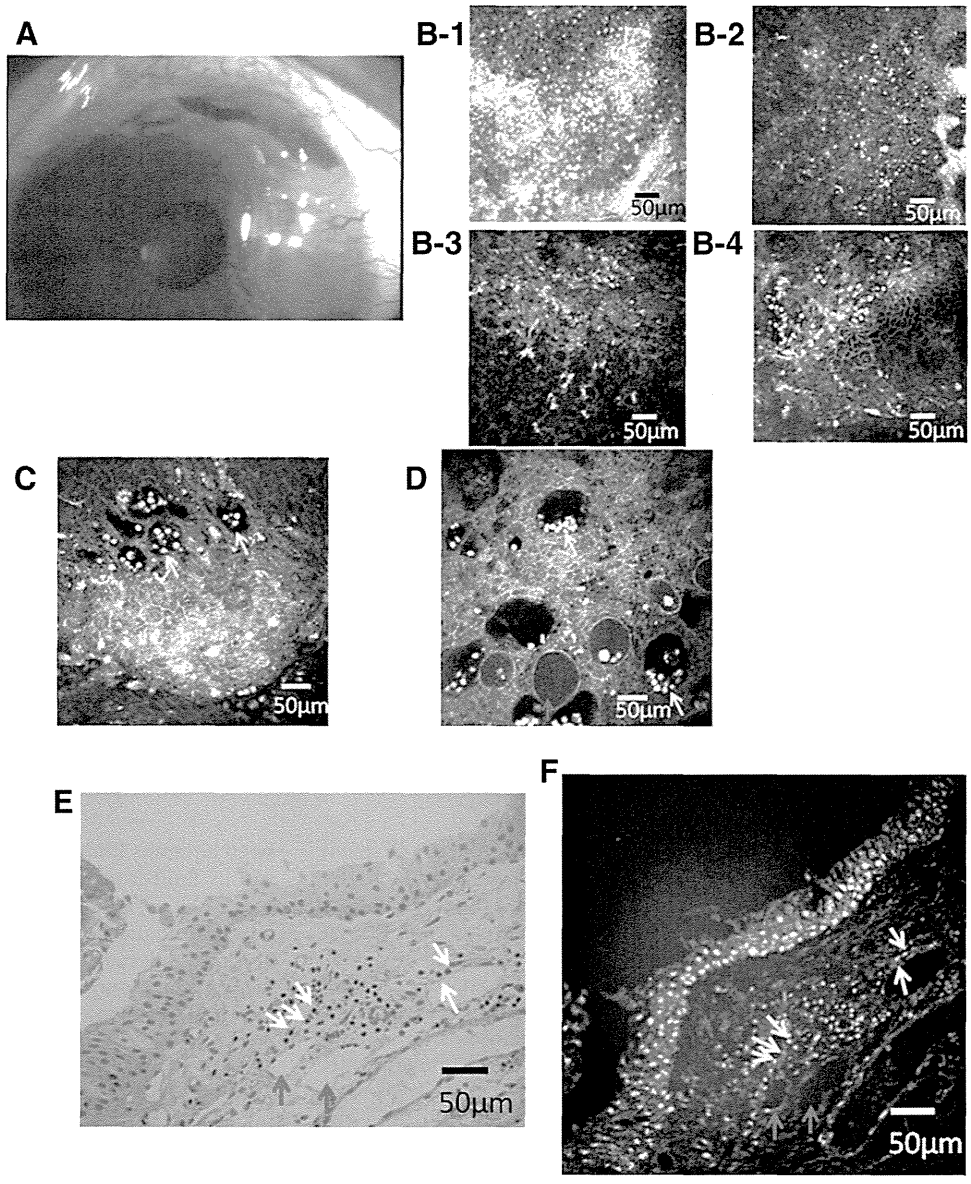

FIGURE 2. Slit lamp microscopy examination, in vivo laser scanning confocal microscopy, and histologic findings in the left eye of patient 4 (eye 5). (**A**) Corneal ulcer with 120° of limbal involvement. (**B**) Corneal findings by in vivo laser scanning confocal microscopy 1 day before corneal perforation (**B-1**, limbal side; **B-2**, central side; **B-3**, superior edge; **B-4**, inferior edge). (**C**) Dark cysts filled with inflammatory infiltrates (*yellow arrows*) in limbal subconjunctiva. (**D**) Fluid-filled cysts (*red arrows*) appeared, as well as dark cysts harboring polymorphs (*yellow arrows*). (**E**) Histologic findings in conjunctiva obtained by conjunctival excision (hematoxylin and eosin staining). (**F**) In vivo confocal microscopy finding in the same specimen shown in (**E**). Note that confocal microscopy effectively discerned features such as cysts (*red arrows*) and inflammatory cells (*yellow arrows*). Magnification: (**E**) ×100.

eration, senile furrow degeneration, ocular rosacea, and leukemia.[6] Pathologically, resected conjunctiva and limbal cornea specimens from subjects with Mooren's ulcer show a large number of plasma cells, lymphocytes, histiocytes, plasma cells, and macrophages.[2,19,20] Schaap et al.[21] reported that circulating autoantibodies in the IgG immunoglobulin class in human corneal epithelium were seen in the serum of patients with Mooren's ulcer. Brown et al.[22] demonstrated the presence of circulating antibodies in both the conjunctival and corneal epithelium in the sera of patients with Mooren's ulcer. Once the diagnosis is established, the only means of following up the course of the disease and/or the treatment responses is by a careful slit lamp examination and detection of circulating antibodies. Histopathologic specimens in patients undergoing conjunctival excision added to our understanding of the disease pathogenesis in Mooren's ulcers (Fig. 2).

The ICD of eyes at the enrollment visit, day 0, showed a strong correlation with the extent of limbal involvement with ulcers measured at the slit lamp microscopic examination (R^2 = 0.8199). Although conjunctival histopathologic alterations have been reported extensively, PubMed and MedLine searches using the key words "in vivo confocal microscopy" and "Mooren's ulcer" revealed no studies in the literature.

In vivo confocal microscopy examination in all patients with Mooren's ulcer showed variable degrees of keratoconjunctival inflammation, with a greater extent of inflammatory cell infiltrates in patients with active ulcers. As we mentioned, we counted only white round cells of 5- to 15-μm diameter. At the basal cell layer level, epithelial cell nuclei are not highly reflective, and so we believe that inflammatory cells could be differentiated from epithelial cell nuclei in that location. The inflammatory cell infiltrates consist of dendritic cells and polymorphs. Since dendritic cells may be mistaken for melanocytes,[16] we chose not to include them in the total count of inflammatory cells, which represents total polymorph densities. It should also be noted that since confocal microscopy diagnosis of an inflammatory cell is based mainly on size, we found it to be logical to refrain from specifying the type of inflammatory cells and thus collectively refer to them as polymorphs. Inflammatory cells in excision specimens from patients with Mooren's ulcers have been reported to consist of neutrophils, lymphocytes, natural killer cells, and monocytes.[20] Further confocal microscopy studies comparing inflammatory cell size and density scan information with size and density of differential inflammatory cell counts in excision specimens would provide invaluable information.

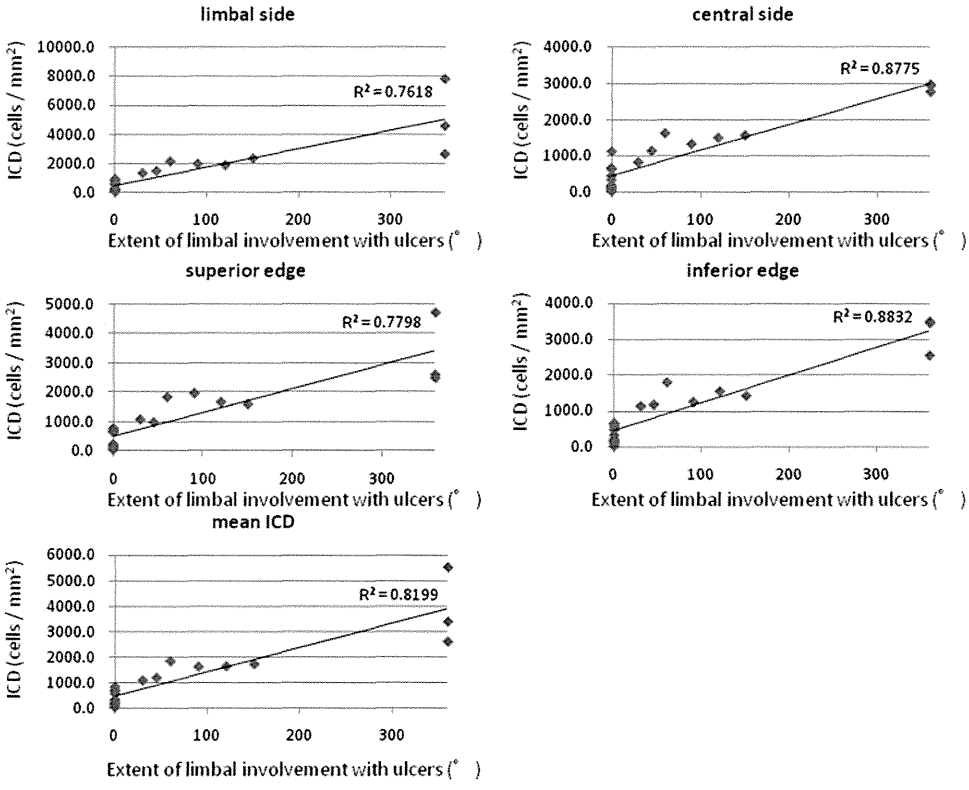

FIGURE 3. The correlation of the ICD of patients' eyes at day 0, and the extent of limbal involvement with ulcers measured by slit lamp microscopy examination. Pearson's correlation analysis revealed that the correlation was very strong.

Dark cysts harboring polymorphs were seen in six of seven patients with active ulcers. Such cysts were not observed in the patients in remission. ICD showed a time-wise decrease with treatment in all patients. The extent of decrease was less in patients 4 and 5, who eventually underwent conjunctival excision. It was noteworthy in the in vivo confocal microscopy observation performed on the day before perforation in patient 4 that the limbal conjunctiva contained two types of subconjunctival cysts: dark cysts, harboring numerous polymorphs that had presented from day 0, and fluid-filled cysts, harboring polymorphs that appeared 1 day before perforation. It is our belief that the fluid in the cysts before perforation might have been aqueous humor oozing through melting corneal tissue or serous fluid from the necrotic tissues. Observation of numerous cysts, especially the fluid-filled variety, may very well suggest imminent perforation and appears to be an important confocal microscopy finding. Since perforation in Mooren's ulcer is rare and since building up more evidence on this important finding is a challenge, observation in this perforated case, we believe, should serve as an open call to all corneal specialists who have access to in vivo confocal microscopy to pay close attention to the changes in the nature of the cysts and their relation to imminent perforation in patients with Mooren's ulcers. Ex vivo confocal microscopy examination of conjunctival histopathologic specimens showed the same architecture in the corresponding areas and revealed the intraepithelial and inflammatory cell infiltrates. ICD in confocal microscopy has been shown to correlate with the severity of ocular surface findings in Sjögren syndrome, atopic keratoconjunctivitis, and meibomian gland dysfunction.[16-18]

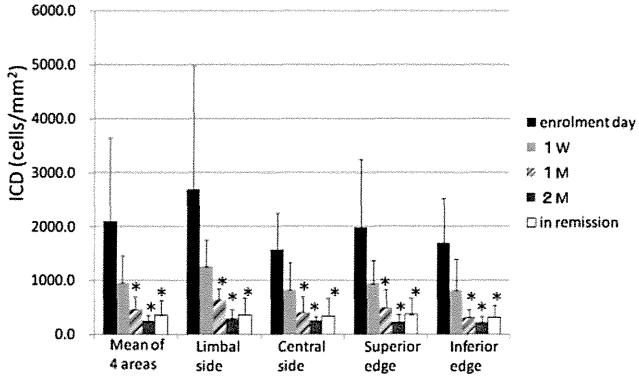

FIGURE 4. The course of ICD change in eyes with active ulcer in response to treatments, compared with the ICD in eyes in remission. Eyes 9 and 10 of patient 7 are excluded this figure, because he was lost to follow-up. The ICD of limbal side, central side, superior edge, inferior edge, and mean of these four sites, of eyes with active ulcer gradually decreased to the same level of ICD of eyes in remission with the treatment. Data are the mean ± SD of ICD values. *Statistically significant compared with the ICD at enrollment day ($P < 0.05$, Student's t-test).

In the present study, eyes with active Mooren's ulcer were managed with aggressive treatment including hourly topical corticosteroids, topical cyclosporine, systemic corticosteroids and cyclosporine, conjunctival excision, and/or keratoepitheliolplasty. It took 4 weeks for the ICD to decrease significantly compared with day 0, and it took 8 weeks to achieve the same level of the ICD in eyes in remission.

ICD assessment adds to our armamentarium of currently existing subjective and objective diagnostic skills in judging the responsiveness of Mooren's ulcer to treatment, including evaluation of the changes in pain symptoms and slit lamp evidence of healing.

In summary, we report the first in vivo confocal scanning laser microscopy study to elucidate the keratoconjunctival alterations in Mooren's ulcer. The study provided evidence that ICD was a useful procedure in evaluating the severity of ulcers and responses to treatment. Observation of numerous limbal cysts, especially fluid-filled cysts may imply imminent perforation, which necessitates a careful follow-up of such patients.

References

1. Zaidman GW, Mondino BJ. Mooren's ulcer. In: Krachmer JH, Mannis MJ, Holland EJ, eds. *Cornea.* 2nd ed. London: Elsevier Mosby; 2005:1241-1244.
2. Brown SI. Mooren's ulcer: histopathology and proteolytic enzymes of adjacent conjunctiva. *Br J Ophthalmol.* 1975;59:670-674.
3. Brown SI, Mondino BJ. Therapy of Mooren's ulcer. *Am J Ophthalmol.* 1984;98:1-6.
4. Wakefield D, Robinson LP. Cyclosporine therapy in Mooren's ulcer. *Br J Ophthalmol.* 1987;71:415-417.
5. Foster CS. Systemic immunosuppressive therapy for progressive bilateral Mooren's ulcer. *Ophthalmology.* 1985;92:1436-1439.
6. Sangwan VS, Zafirakis P, Foster CS. Mooren's ulcer: current concepts in management. *Indian J Ophthalmol.* 1997;45:7-17.
7. Martin NF, Stark WJ, Maumenee AE. Treatment of Mooren's and Mooren's-like ulcer by lamellar keratectomy: report of six eyes and literature review. *Ophthalmic Surg.* 1987;18:564-569.
8. Kinoshita S, Ohashi Y, Ohji M, et al. Long-term results of keratoepithelioplasty in Mooren's ulcer. *Ophthalmology.* 1991;98:438-445.
9. Solomon A, Meller D, Prabhasawat P, et al. Amniotic membrane grafts for nontraumatic corneal perforations, descemetoceles, and deep ulcers. *Ophthalmology.* 2002;109:694-703.
10. Brown SI, Mondino BJ. Penetrating keratoplasty in Mooren's ulcer. *Am J Ophthalmol.* 1980;89:255-258.
11. Kaufman SC, Musch DC, Belin MW, et al. Confocal microscopy; a report by the American Academy of Ophthalmology. *Ophthalmology.* 2004;111:396-406.
12. Matsumoto Y, Dogru M, Sato EA, et al. The application of in vivo confocal scanning laser microscopy in the management of Acanthamoeba keratitis. *Mol Vis.* 2007;13:1319-1326.
13. Kobayashi A, Yoshita T, Sugiyama K. In vivo findings of the bulbar/palpebral conjunctiva and presumed meibomian glands by laser scanning confocal microscopy. *Cornea.* 2005;24:985-988.
14. Messmer EM, Torres Suarez E, Mackert MI, et al. In vivo confocal microscopy in blepharitis. *Klin Monatsbl Augenheilkd.* 2005;222:894-900.
15. De Nicola R, Labbe A, Amar N, et al. In vivo confocal microscopy and ocular surface disease: anatomical-clinical correlations (in French). *J Fr Ophtalmol.* 2005;28:691-698.
16. Wakamatsu TH, Sato EA, Matsumoto Y, et al. Conjunctival in vivo confocal scanning laser microscopy in patients with Sjögren syndrome (SS). *Invest Ophthalmol Vis Sci.* 2010;51:144-150.
17. Hu Y, Sato EA Matsumoto Y, et al. Conjunctival in vivo confocal scanning laser microscopy in patients with atopic keratoconjunctivitis. *Mol Vis.* 2007;13:1379-1389.
18. Matsumoto Y, Sato EA, Osama MA, et al. The application of in vivo laser confocal microscopy to the diagnosis and evaluation of meibomian gland dysfunction. *Mol Vis.* 2008;14:1263-1271.
19. Young RD, Watson PG. Light and electron microscopy of corneal melting syndrome (Mooren's ulcer). *Br J Ophthalmol.* 1982;66:341-356.
20. Lopez JS, Price FW, Whitcap SM, et al. Immunohistochemistry of Terrien's and Mooren's corneal degeneration. *Arch Ophthalmol.* 1991;109:988-992.
21. Schaap OL, Feltkamp TEW, Breebaart AC. Circulating antibodies to corneal tissue in a patient suffering from Mooren's ulcer (ulcus rodens corneae). *Clin Exp Immunol.* 1969;5:365-370.
22. Brown SI, Mondino BJ, Rabin BS. Autoimmune phenomenon in Mooren's ulcer. *Am J Ophthalmol.* 1976;82:835-840.